Effect of Electric Field on the Optically Detected Quantum Magnetophonon Resonances in Semiconductors in a Quantized Magnetic Field

Sang Chil Lee* and Jeong Woo Kang**

Abstract

The frequency-dependent magnetoconductivity is applied to bulk polar semiconductors and the optically detected quantum magnetophonon resonance (OQDMPR) conditions are obtained. The qualitative features of the ODQMPR effects are investigated as a function of the strength of magnetic field and the strength of the electric field. In particular, anomalous behaviors of the ODQMPR lineshape such as the changes in the ODQMPR amplitude, the appearance of the antiresonances in the ODQMPR lineshape under the quantum magnetophonon resonance(QMPR) condition, the disappearance of the antiresonances under the dc electric field, and the splitting and the shift of the ODQMPR peaks are discussed in detail.

Keywords: Magnetoconductivity, Quantum magnetophonon resonance, Optically detected quantum magnetophonon resonance, Antiresonance

I. Introduction

The quantum magnetophonon resonance (QMPR) effect predicted by Gurevich and Firsov [1] in bulk and low-dimensional semiconductor systems [2-10] has been studied in considerable detail from both the experimental and theoretical points of views because the

* Department of Physics, Cheju National University, Jeju, Korea
** Department of Science Education, Cheju National University, Jeju, Korea

QMPR effect is powerful spectroscopic tools to investigate various transport properties of semiconductors. Under a magnetic field, the QMPR effect arises from resonant scattering of the electrons in Landau levels by longitudinal optical (LO) phonons whenever the phonon energy is equal to an integral multiple of energy difference between two of Landau levels. The QMPR provides useful information on band structure parameters, such as the carrier relaxation mechanism, damping of the oscillations due to the electron-phonon interaction, the phonon frequencies, the effective mass, and the energy levels. Thus, many studies of the QMPR effect has been reported [4-10]. Especially, since their properties are very sensitive to the type of scattering mechanisms, the shape of the line, the linewidth and the shift of the QMPR peaks, the dependence of temperature and magnetic field strength were the object of study. However, the QMPR can also be observed directly through a linewidth and effective mass of the electron cyclotron resonance (CR), as was demonstrated in three-dimensional (3D) semiconductor systems of GaAs by Hai and Peeters [11] and in two-dimensional (2D) semiconductor systems of $GaAs/Al_xGa_{1-x}As$ heterojunctions by Barnes et al. [12]. The optically detected QMPR(ODQMPR) allows one to make quantitative measurements of the scattering strength for specific Landau levels and yields direct information on the nature of the electron-phonon interaction in semiconductors.

In this paper, we apply the frequency-dependent magnetoconductivity, which is obtained by using the Mori-type projection operator technique [13], to bulk polar semiconductor, n-InSb, and investigate the features of the optically detected magnetophonon resonances as a function of the incident photon frequency, the strength of magnetic field, and the strength of the electric field in such a material. In particular, the appearance of the antiresonances in the electric-field-induced ODQMPR line shape near CR main peaks under the condition MPR, the disappearance of the antiresonances under the Dc electric field, and the splitting and the shift of the electric-field-induced ODMPR peaks are obtained.

The rest of the paper is organized as follows: In Sec. II, we present our theoretical formulations of the problem. Numerical results for the magnetoconductivity of n-InSb are presented in Sec. III. In particular, the electric-field-induced ODQMPR conditions for the model system is given, and the effect of the incident photon frequency, the temperature, and the strength of magnetic field on the electric-field-induced ODQMPR are discussed. Here, special attention is given to the anomalous behavior of the electric-field-induced ODQMPR line shape, such as the appearance of the antiresonances in the electric-field-induced ODQMPR line shape near CR main peaks and the height and width of the electric-field-induced ODMPR peaks. Our results are summarized in the last section.

Ⅱ. THEORETICAL FRAMEWORK

A system of many noninteracting electrons N_e in interaction with phonons is considered initially in equilibrium with a temperature T. Then, in the presence of a uniform electric field $\boldsymbol{F} = (F, 0, 0)$ and a constant magnetic field $\boldsymbol{B} = (0, 0, B)$, the time-independent Hamiltonian H of the system can be expressed as

$$H = \sum_{\lambda}\sum_{\lambda'}\langle\lambda|(h_e + v)|\lambda'\rangle a_{\lambda}^{+} a_{\lambda'} + H_p, \tag{1}$$

$$h_e = \frac{1}{2m^*}(\boldsymbol{p} + e\boldsymbol{A})^2 + eFx, \tag{2}$$

$$v = \sum_{q}[C_q^{+} b^{+} \exp(-i\boldsymbol{q}\cdot\boldsymbol{r}) + C_q b_q \exp(i\boldsymbol{q}\cdot\boldsymbol{r})], \tag{3}$$

$$H_p = \sum_{q}\hbar\omega_q(b_q^{+} b_q + \frac{1}{2}), \tag{4}$$

where $|\lambda\rangle$ means the Landau state $|N, \boldsymbol{k}\rangle$ in the conduction band, and $N(=0, 1, 2, \cdots)$ is the Landau-level index, $a_{\lambda}^{+}(a_{\lambda})$ is the creation (annihilation) operator for an electron with effective mass m^* and momentum $\boldsymbol{p}$, $\boldsymbol{A}$ is the vector potential, $b_q^{+}(b_q)$ is the creation (annihilation) operator for a phonon with momentum $\hbar\boldsymbol{q}$ and energy $\hbar\omega_q$, C_q is the interaction operator, and $\boldsymbol{r}$ is the position vector of an electron. By taking into account the Landau guage of vector potential $\boldsymbol{A} = (0, Bx, 0)$ the one-electron normalized eigenfuncitons ($\langle \boldsymbol{r} | N, k_y, k_z\rangle$) and eigenvalues ($E_{\lambda}$) in the conduction band are obtained by

$$\langle \boldsymbol{r} | N, k_y, k_z\rangle = \frac{1}{\sqrt{L_y L_z}}\Phi_N(x - x_0)\exp(ik_y y + ik_z z), \tag{5}$$

$$E_{\lambda} = E_N(k_y, k_z) = \left(N + \frac{1}{2}\right)\hbar\omega_c + \frac{\hbar^2 k_z^2}{2m^*} - \hbar V_d k_y - \frac{1}{2}m^* V_d^2, \tag{6}$$

where $x_0 = -l_B^2(k_y + eF/\hbar\omega_c)$ with $l_B = \sqrt{\hbar/m^*\omega_c}$, ,$ k_y and k_z are the wave vector component of the electron in the x and z direction, respectively, $\omega_c(= eB/m^*)$ is the cyclotron frequency in the conduction band, V_d is the drift velocity of the electron, $\Phi_N(x)$ in Eq. (5) is the eigenfunction of the simple harmonic oscillator, and L_y and L_z are, respectively, the y- and z-directional normalization lengths.

When a linearly polarized electromagnetic wave of amplitude E and frequency ωgiven by

$$E_x = E\cos\omega t,\ E_y = 0,\ E_z = 0 \tag{7}$$

is applied along the z axis, the absorption power delivered to the system is given for the Faraday configuration ($E \perp B$) as [13,14]

$$P = \frac{E^2}{2}\,\bar{\sigma}_{xx}(\omega), \tag{8}$$

where $\bar{\sigma}_{xx}(\omega) = (\sigma_{xx}(\omega) + \sigma_{xx}(-\omega))/2$ and $\sigma_{xx}(\omega)$ (or $\sigma_{xx}(-\omega)$) is the frequency-dependent magnetoconductivity corresponding to the right- (or left-) circularly polarized wave, and can be expressed as [13,14]

$$\sigma_{xx}(\omega) = \frac{\hbar}{V}\sum_{\lambda',\lambda} \left|\langle\lambda|j_x|\lambda'\rangle\right|^2 \frac{f(E_{\lambda'}) - f(E_\lambda)}{E_{\lambda'} - E_\lambda} S_{\lambda'\lambda}, \tag{9}$$

where the field-dependent spectral density $S_{\lambda'\lambda}$ is given by

$$S_{\lambda'\lambda} = \frac{\hbar\Gamma_{\lambda'\lambda}(\omega)}{[\hbar\omega - E_{\lambda'} + E_\lambda - \hbar\nabla_{\lambda'\lambda}(\omega)]^2 + \hbar^2\Gamma^2_{\lambda'\lambda}(\omega)} \tag{10}$$

for any localized quantum states λ' and λ. Here V represents the volume of the system, j_x is the x component of the single-electron current operator, $f(E_\lambda)$ is a Fermi-Dirac distribution function associated with the eigenstate $|\lambda\rangle$ of Eq. (5) and the eigenvalue E_λ of Eq. (6). Also $\nabla_{\lambda'\lambda}(\omega)$ and $\Gamma_{\lambda'\lambda}(\omega)$ are, respectively, the field-dependent line shift and the field-dependent relaxation rate in the spectral line shape due to collisions associated with the transition arising from the resonant absorption or emission of a single photon of frequency ω and of a single phonon of frequency ω_q between states $|\lambda\rangle$ and $|\lambda'\rangle$. The field-dependent line shift $\nabla_{\lambda'\lambda}(\omega)$ provides the resonance shifting and the field-dependent relaxation rate $\Gamma_{\lambda'\lambda}(\omega)$ gives directly the average value of the relaxation time τ ($\sim\Gamma_{\lambda'\lambda}(\omega)/\hbar$), whereas the inverse of which measures the broadening of the absorption resonance spectrum. It should be noted that both of these quantities depend on the temperature, the magnetic field, impurity concentration, and the incident photon frequency.

To obtain the frequency-dependent magnetoconductivity $\sigma_{xx}(\omega)$ of Eq. (9) for the present model system given in Eqs. (5) and (6), we need the matrix elements of the x -component single-electron current operator $|\langle Nk_yk_z|j_x|N'k_y'k_z'\rangle|^2$ given by

$$|\langle Nk_yk_z|j_x|N'k_y'k_z'\rangle|^2 = \frac{e^2\hbar\omega_c}{2m^*}[(N+1)\delta_{N+1N'}+N\delta_{N-1N'}]\delta_{k_y,k_y'}\delta_{k_z,k_z'} \quad (11)$$

where $j_x = -ep_x/m^*$ and the Kronecker symbols ($\delta_{NN'}, \delta_{k_y,k_y'}, \delta_{k_z,k_z'}$) denote the selection rules, which arise from the integration of the matrix elements with respect to each direction. We also replace summations with respect to k_y and k_z in $\sum_{N,k_y,k_z}$ by the following relation [7]:

$$\sum_{k_y,k_z}(\cdots) = \frac{L_yL_z}{4\pi^2}\int_{-m^*\omega_cL_x/2\hbar-eF/\hbar\omega_c}^{m^*\omega_cL_x/2\hbar-eF/\hbar\omega_c}dk_y\int_{-\pi/L_z}^{\pi/L_z}dk_z(\cdots). \quad (12)$$

In addition, we assume that the fs in Eq. (9) can be replaced by the Boltzmann distribution function for nondegenerate semiconductor [7], i.e., $f[E_N(k_y,k_z)] \approx \exp\{\beta[\mu-E_N(k_y,k_z)]\}$, where $\beta = 1/k_BT$ with k_B being Boltzmann constant and T temperature, and μ denotes the chemical potential given by $\mu=(1/\beta)\ln\left[\frac{(2\pi^3n_e^2L_x^2\beta^3\hbar^4V_d^2/m^*)^{1/2}\exp(\beta m^*V_d^2/2)\sinh(\beta\hbar\omega_c/2)}{\sinh(\beta m^*\omega_cV_dL_x/2)}\right]$. Here $n_e = N_e/V$ denotes the electron density. Then, the frequency-dependent magnetoconductivity $\sigma_{xx}(\omega)$ corresponding to the right-circularly polarized wave is obtained as follows

$$\frac{\sigma_{xx}(\omega)}{\sigma_0} = \sum_{N=0}^{\infty} A_N(\omega) S_N(\omega), \tag{13}$$

where the amplitude factor is

$$A_N(\omega) = \sqrt{\frac{\pi\beta}{2m^*\tau^2}}(N+1)\sinh\left(\frac{1}{2}\beta\hbar\omega_c\right)\left(1-e^{-\beta\hbar\omega_c}\right)e^{-\beta\left(N+\frac{1}{2}\right)\hbar\omega_c} \tag{14}$$

and the averaged Lorentzian spectrum function is defined as

$$S_N(\omega) = \frac{1}{\pi}\int_{1st\,BZ} e^{-\frac{\beta\hbar^2 k_z^2}{2m^*}} \frac{\hbar\Gamma_{N+1,k_y,k_z;N,k_y,k_z}(\omega)}{(\hbar\omega-\hbar\omega_c)^2+\hbar^2\Gamma^2_{N+1,k_y,k_z;N,k_y,k_z}(\omega)}\, dk_z. \tag{15}$$

S_N has a form of the Boltzmann average of the spectral density for a shift of zero, $\nabla \simeq 0$, in the spectral line shape. Here $\sigma_0 = e^2 n_e \tau/m^*$ with τ being static relaxation time in the absence of a photon. We could see that the frequency-dependent magnetoconductivity in Eq. (13) exhibits a Lorentzian line shape.

An analytical expression of the relaxation rates in Eq. (15) in the lowest-order approximation for the weak electron-phonon interaction can be evaluated from the general expression of the field-dependent relaxation rates given by Eq. (4.6) of Ref. 13. With the help of Eq. (6), the field-dependent relaxation rate associated with the electronic transition between the states $|N+1, k_y, k_z\rangle$ and $|N, k_y, k_z\rangle$ is expressed by

$$\Gamma_{N+1,k_y,k_z;N,k_y,k_z}(\omega) = \Gamma^+_{N+1,k_y,k_z;N,k_y,k_z}(\omega) + \Gamma^-_{N+1,k_y,k_z;N,k_y,k_z}(\omega), \tag{16a}$$

$$\begin{aligned}
&\Gamma^+_{N+1,k_y,k_z;N,k_y,k_z}(\omega) \\
&= \pi\sum_q \sum_{N'\neq N+1} |C(q)|^2 |J_{N+1,N'}(q_\perp)|^2 \\
&\times\left\{(1+n_q)\delta\left[\hbar\omega+(n-n')\hbar\omega_c+\frac{\hbar^2k_z^2}{2m^*}-\frac{\hbar^2(k_z-q_z)^2}{2m^*}-\hbar q_y V_d-\hbar\varpi_{\vec{q}}\right]\right. \\
&\left.+n_q\delta\left[\hbar\omega+(n-n')\hbar\omega_c+\frac{\hbar^2k_z^2}{2m^*}-\frac{\hbar^2(k_z+q_z)^2}{2m^*}+\hbar q_y V_d+\hbar\varpi_{\vec{q}}\right]\right\},
\end{aligned} \tag{16b}$$

$$\begin{aligned}&\Gamma^{-}_{N+1,k_y,k_z;N,k_y,k_z}(\omega)\\&=\pi\sum_{q}\sum_{N'\neq N}|C(q)|^2|J_{N,N'}(q_\perp)|^2\{(1+n_q)\\&\times\delta\left[\hbar\omega+(n'-n-1)\hbar\omega_c-\frac{\hbar^2k_z^2}{2m^*}+\frac{\hbar^2(k_z+q_z)^2}{2m^*}-\hbar q_yV_d+\hbar\varpi_{\vec{q}}\right]\\&+n_q\delta\left[\hbar\omega+(n'-n-1)\hbar\omega_c-\frac{\hbar^2k_z^2}{2m^*}+\frac{\hbar^2(k_z-q_z)^2}{2m^*}+\hbar q_yV_d-\hbar\varpi_{\vec{q}}\right]\Bigg\},\end{aligned}\tag{16c}$$

where N' indicates the intermediate localized Landau level indices, $n_q = [\exp(\beta\hbar\omega_q)-1]^{-1}$ is the phonon distribution function, C_q is the Fourier transform of the electron-ohonon interaction potential, and

$$|J_{N,N'}(u_\perp)|^2 = \frac{N_{\langle}!}{N_{\rangle}!}\exp[-u_\perp]u_\perp^{\Delta N}[L_{N_\langle}^{\Delta N}(u_\perp)]^2,\tag{17}$$

where $u_\perp = l_B^2q_\perp^2/2$ with $q_\perp^2 = q_x^2+q_y^2$.. Here, $N_\langle = \min\{N,N'\}$, $N_\rangle = \max\{N,N'\}$, and $L_{N_\langle}^{\Delta N}(u_\perp)$ is an associated Laguerre polynomial [16] with $\Delta N = N_\rangle - N_\langle$.

To calculate the field-dependent relaxation rates Γ of Eq. (16) for electron-phonon interactions, we consider the Fourier component of the interaction potentials[7] for polar LO-phonon scattering given by $|C(q)|^2 = D'/(\Omega q^2)$ with D' being the constant of the polar interaction, where the assumption that the phonons are dispersionless (i.e., $\hbar\omega_{\vec{q}} \approx \hbar\omega_{LO} \approx$ constant, where ω_{LO} is the longitudinal optical phonon frequency) was made. As shown in Eq. (16), the relaxation rates Γ involves integrations with respect to q_x, q_y, and q_z in Cartesian coordinates. The integral over q_x, q_y, and q_z is very difficult to evaluate analytically since it must be done separately for each N and N'. So, to simplify the calculations, we replace $\hbar q_yV_d$ in the argument of the δfunction by the potential energy difference $eF\Delta\bar{y}$ across the spatial extent $\Delta\bar{y}$ of a Landau state as some authors did [17,18]. Then, the field-dependent relaxation rates associated with the electronic transition between the states $|N+1,k_y,k_z\rangle$ and $|N,k_y,k_z\rangle$ can be expressed as

$$
\begin{aligned}
&\Gamma\ (N+1, k_y, k_z : N, k_y, k_z) \\
&= \frac{D'}{4\pi}\sqrt{\frac{m^*}{2\hbar^2}}\ \sum_{N' \neq N}\sum_{\pm}(n_q+1) \\
&\times\left(\frac{K_1^{\pm}(N,N';k_z)\Theta(\Theta_1(k_z))}{\sqrt{\Theta_1(k_z)}}+\frac{K_3^{\pm}(N,N';k_z)\Theta(\Theta_3(k_z))}{\sqrt{\Theta_3(k_z)}}\right) \\
&+n_q\left(\frac{K_2^{\pm}(N,N';k_z)\Theta(\Theta_2(k_z))}{\sqrt{\Theta_2(k_z)}}+\frac{K_4^{\pm}(N,N';k_z)\Theta(\Theta_4(k_z))}{\sqrt{\Theta_4(k_z)}}\right),
\end{aligned} \tag{18}
$$

where $\Theta(x)$is the Heaviside step function defined by $\Theta(x) = 1$ for $x \geq 0$ and 0 for $x < 0$,

$$\Theta_1(k_z) = \hbar\omega + (N-N')\hbar\omega_c + \frac{\hbar^2 k_z^2}{2m^*} - eF\sqrt{\hbar m^* \omega_{LO}} - \hbar\omega_{LO}, \tag{19a}$$

$$\Theta_2(k_z) = \hbar\omega + (N-N')\hbar\omega_c + \frac{\hbar^2 k_z^2}{2m^*} + eF\sqrt{\hbar m^* \omega_{LO}} + \hbar\omega_{LO}, \tag{19b}$$

$$\Theta_3(k_z) = \hbar\omega + (N'-N-1)\hbar\omega_c + \frac{\hbar^2 k_z^2}{2m^*} - eF\sqrt{\hbar m^* \omega_{LO}} + \hbar\omega_{LO}, \tag{19c}$$

$$\Theta_4(k_z) = \hbar\omega + (N'-N-1)\hbar\omega_c + \frac{\hbar^2 k_z^2}{2m^*} + eF\sqrt{\hbar m^* \omega_{LO}} - \hbar\omega_{LO}, \tag{19d}$$

and

$$K_1^{\pm}(N,N';k_z) = \frac{1}{2}\int_0^{\infty} du_\perp |J_{N+1,N'}(u_\perp)|^2 \frac{1}{u_\perp + l_B^2\left(k_z \pm \sqrt{2m^*\Theta_1(k_z)/\hbar^2}\right)^2/2}, \tag{20a}$$

$$K_2^{\pm}(N,N';k_z) = \frac{1}{2}\int_0^{\infty} du_\perp |J_{N+1,N'}(u_\perp)|^2 \frac{1}{u_\perp + l_B^2\left(k_z \pm \sqrt{2m^*\Theta_2(k_z)/\hbar^2}\right)^2/2}, \tag{20b}$$

$$K_3^{\pm}(N,N';k_z) = \frac{1}{2}\int_0^{\infty} du_\perp |J_{N,N'}(u_\perp)|^2 \frac{1}{u_\perp + l_B^2\left(k_z \pm \sqrt{2m^*\Theta_3(k_z)/\hbar^2}\right)^2/2}, \tag{20c}$$

$$K_4^{\pm}(N,N';k_z) = \frac{1}{2}\int_0^{\infty} du_\perp |J_{N,N'}(u_\perp)|^2 \frac{1}{u_\perp + l_B^2\left(k_z \pm \sqrt{2m^*\Theta_4(k_z)/\hbar^2}\right)^2/2}. \tag{20d}$$

In order to obtain Eq. (18), we transformed the sum over q in Eq. (16) into an integral form in the usual way as $\sum_q \rightarrow (V/(2\pi)^3)\int_{-\infty}^{\infty}\int_{-\infty}^{\infty}\int_{1st\,BZ} dq_x dq_y dq_z$ and used the following property of the Dirac delta function: $\delta[f(x)] = \sum_i \delta[x-x_i]/|f'(x_i)|$ with x_i being the roots of $f(x)$, and the approximaton [17,18] $eF\Delta\bar{y} \approx eF\sqrt{\hbar/m^*\omega_{LO}}$. It is clearly seen from Eq. (16) that the relaxation rates diverge whenever the conditions $\Theta_i(k_z) = 0$ and $a^2_{i\pm} = 0$ in $K_i^{\pm}(N,N';t)$ are satisfied. From these conditions, the frequency-dependent magnetoconductivities $\sigma_{xx}(\omega)$ for polar LO-phonon scattering show the resonant behaviors at $P\hbar\omega_c \pm \hbar\omega = \hbar\omega_{LO} \pm eF\sqrt{\hbar/m^*\omega_{LO}}$ $(P \equiv N'-N = 1,2,3,..)$. When the electric-field-induced ODQMPR conditions are satisfied in the course of scattering events, the electrons in the Landau levels specified by the level index (N) can make transitions to one of the Landau levels (N') by absorbing and/or emitting a photon of energy $\hbar\omega$ during the absorption of a LO phonon of energy $\hbar\omega_{LO}$. Equation (13), together with Eq. (15), is the basic equation for the electric-field-induced ODMPR spectral line shape, which enables us to analyze the electric-field-induced ODQMPR effects in semiconductors under magnetic fields.

III. NUMERICAL RESULTS AND DISCUSSIONS

In this section, we present the numerical results of the frequency-dependent magnetoconductivity formula $\bar{\sigma}_{xx}(\omega)$ in Eq. (8), together with Eq. (16), which is related to the electric-field-induced ODQMPR for the bulk materials. Here, special attention is given to the behavior of the electric-field-induced ODQMPR line shape, such as the appearance of the electric-field-inducedODQMPR peaks and the shift of the electric-field-induced ODQMPR peaks. For our numerical results of Eqs. (8) and (16), the parameters of n-InSb are taken [19,20] by an effective mass $m^* = 0.014m_0$ with m_0 being the electron rest mass, a LO-phonon energy $\hbar\omega_{LO} = 24.4$ meV, the electron density $n_e = 4\times10^{24}\ \mathrm{m}^{-3}$ and the constant of the polar interaction $D' = 5.2\times10^{-50}\ \mathrm{kg^2m^7s^{-4}}$. In addition, twenty-one Landau levels are included in the calculation of the frequency-dependent magnetoconductivity.

Figure 1 shows the electric-field strength dependence of the magnetoconductivities $\bar{\sigma}_{xx}(\omega)$ as a function of the magnetic strength for the different photon frequencies of polar material n-InSb. As shown in Fig. 1, the various peaks are observed for the various different strength of magnetic field. It is clearly seen from the figure that main peaks are observed at the value satisfied by the cyclotron resonance condition ($\omega = \omega_c$) and/or the optically

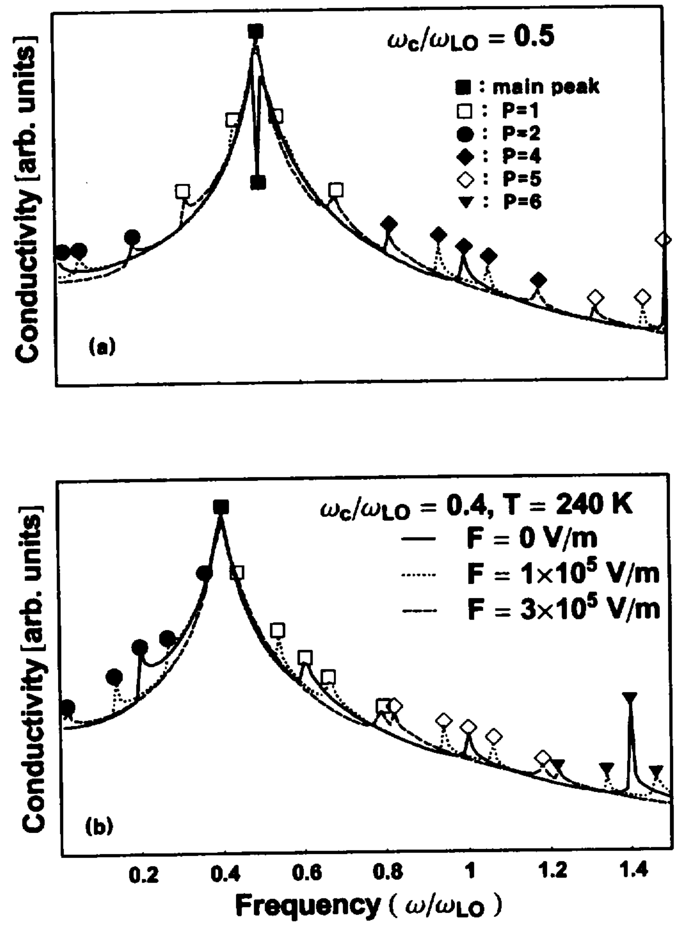

Fig. 1 Electric-field dependence of the magnetoconductivity [$\bar{\sigma}_{xx}(\omega)$] as a function of incident photon frequency for n-InSb at $T = 240$ K.

detected quantum magnetophonon resonance condition given by $P\hbar\omega_c \pm \hbar\omega = \hbar\omega_{LO}$ whereas subsidiary peaks are exhibited at the value satisfied the electric-field-induced ODQMPR condition $P\hbar\omega_c \pm \hbar\omega = \hbar\omega_{LO} \pm eF\sqrt{\hbar/m^*\omega_{LO}}$. Therefore, it is to be noted that all peaks can be obtained from the CR and the electric-field-induced ODQMPR condition. The physical origin of the small dip structure can be understood by considering the field-dependent relaxation rate [11]. The field-dependent relaxation rate increases sharply since the strong coupling of the electron -phonon-photon interaction takes place when the condition $\omega = \omega_c = \omega_{LO}/N$ is satisfied, as a result, the field-dependent magnetoconductivity is clearly reduced. This antiresonance of the field-dependent magnetoconductivity is associated with the fact that, since the electron is fully scattered back and forth between the two Landau levels by the absorption of a single photon of frequency $\omega = \omega_c = \omega_{LO}/N$ and the emission of a LO phonon of frequency $\omega_{LO} = N\omega_c$, an electron is localized at two Landau levels. It is very interesting that the antiresonances (double peak structure) would appear whenever the strong electron-phonon-photon coupling takes place at CR main peaks ($\omega = \omega_c = \omega_{LO}/N$). The appearance of antiresonances in the electric-field-induced ODQMPR line shape seems to be fundamental in the electric-field-induced ODQMPR effects. As the strength of the electric field increases, the width of splitting of the electric-field-induced ODQMPR peaks splitted from the MPR peaks increases. The electric-field-induced ODQMPR peaks ($\omega \neq 0$) obtained from the condition ($P\hbar\omega_c \pm \hbar\omega = \hbar\omega_{LO} \pm eF\sqrt{\hbar/m^*\omega_{LO}}$) are splitted by two different peaks, respectively, under the electric field, and the width of splitted peaks increases with increasing strength of electric field.

Figure 2 shows the electric-field strength dependence of the magnetoconductivities $\bar{\sigma}_{xx}(\omega)$ as a function of photon frequency for the different magnetic field strengths of polar material n-InSb. As shown in Fig. 2, the main peaks obtained from the CR condition ($\omega = \omega_c$) appear at the same photon frequency although the strength of the electric field increases. A double peak appeared around $\omega/\omega_{LO} = 0.5$ for $\omega_{c}/\omega_{LO} = 0.5$ and the small dip observed disappear under the electric field. The splitting of the subsidiary electric-field-induced ODQMPR peaks obtained from the condition ($P\hbar\omega_c \pm \hbar\omega = \hbar\omega_{LO} \pm eF\sqrt{\hbar/m^*\omega_{LO}}$) takes place from QMPR peaks and the width of splitting increases as the strength of the electric field increases. Our results are for the case where a linearly polarized electromagnetic wave is applied to the system. Therefore, the electric-field-induced ODQMPR conditions are given by $P\hbar\omega_c \pm \hbar\omega = \hbar\omega_{LO} \pm eF\sqrt{\hbar/m^*\omega_{LO}}$ and $P\hbar\omega_c \pm \hbar\omega = \hbar\omega_{LO}$, respectively.

In addition, CR peak shifts have been neglected in our result, because we are interested in anomalous behaviors of the electric-field-induced ODQMPR line shape.

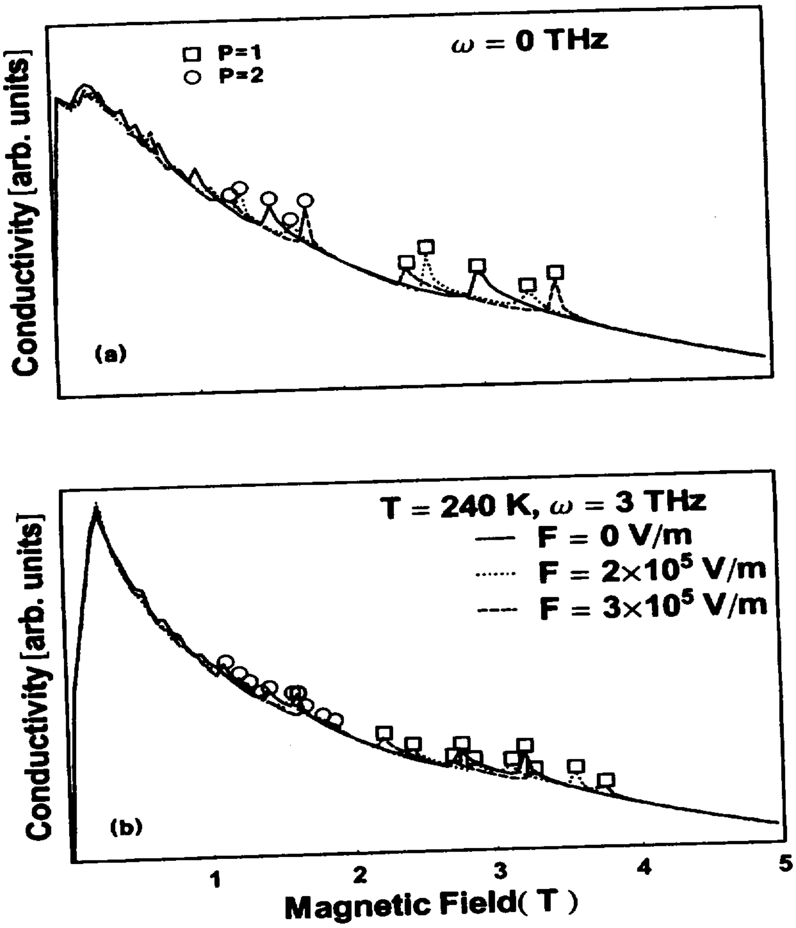

Fig. 2 Electric-field dependence of the magnetoconductivity [$\bar{\sigma}_{xx}(\omega)$] as a function of magnetic field strength for n-InSb at $T = 240K$.

V. CONCLUDING REMARKS

In conclusion, we have derived the frequency-dependent magnetoconductivity $\bar{\sigma}_{xx}(\omega)$ for n-InSb materials and obtained the electric-field-induced ODQMPR conditions by $P\hbar\omega_c \pm \hbar\omega = \hbar\omega_{LO} \pm eF\sqrt{\hbar/m^*\omega_{LO}}$ as a function of the strength of the applied magnetic field (B) and the incident photon frequency (ω) under an electric field. With the electric-field-induced ODQMPR conditions, we have investigated the physical characteristics of the electric-field-induced ODQMPR effects in n-InSb. In particular, we have studied the variation of the anomalous behavior of the electric-field-induced ODQMPR line shape with the splitting and the shift of electric-field-induced ODQMPR peaks, changes of the electric-field-induced ODQMPR amplitude, the appearance of the double peak structure near CR peaks, the disappearance of the double peak under the electric field and the height and width of the electric-field-induced ODQMPR peaks.

Our results show that (1) the antiresonances in the electric-field-induced ODQMPR line shape near CR main peaks ($\omega = \omega_c = \omega_{LO}/N$) are observed. (2) Under the electric field, the main peaks obtained from the CR condition($\omega = \omega_c$) appear at the same photon frequency. A double peak around the small dip observed disappear under the electric field. The splitting of the subsidiary electric-field-induced ODQMPR peaks obtained from the condition($P\hbar\omega_c \pm \hbar\omega = \hbar\omega_{LO} \pm eF\sqrt{\hbar/m^*\omega_{LO}}$) takes place from QMPR peaks and the width of splitting increases as the strength of the electric field increases. (3) The electric-field-induced ODQMPR peaks($\omega \neq 0$) obtained from the condition ($P\hbar\omega_c \pm \hbar\omega = \hbar\omega_{LO} \pm eF\sqrt{\hbar/m^*\omega_{LO}}$) are splitted by two different peaks, respectively, under the electric field, and the width of splitted peaks increases with increasing strength of electric field. In addition, strong oscillations of the magnetoconductivity in bulk materials such as n-InSb are expected in terms of the optically detected quantum magnetophonon resonance, which indicate that the electric-field-induced ODQMPR should also be observed experimentally in such bulk semiconductors. Throughout this work, the single-particle picture has been used. Thus, electron-electron interactions have been ignored. Despite the above shortcomings of the theory, we expect that our results will help to understand the electric-field-induced ODQMPR effects in n-InSb.

References

[1] V. L. Gurevich and Yu A. Firsov, Zh. Eksp. Teor. Fiz. 40, 198 (1961) [Sov. Phys. JETP 13, 137 (1961)].

[2] R. J. Nicholas, Prog. Quantum Electron. 10, 1 (1985).

[3] D. Schneider, C. Brink, G. Irmer, and P. Verma, Physica B 256-258, 625 (1998).

[4] P. Warmenbol, F. M. Peeters, and J. T. Devreese, Phys. Rev. B 39, 7821 (1989); 37, 4694 (1988).

[5] N. Mori, H. Momose, and C. Hamaguchi, Phys. Rev. B 45, 4536 (1992).

[6] J. Y. Ryu and R. F. O'Connell, Phys. Rev. B 48, 9126 (1993); J. Y. Ryu, G. Y. Hu, and R. F. O'Connell, ibid. 49, 10 437 (1994).

[7] A. Suzuki and M. Ogawa, J. Phys. C 10, 4659 (1998).

[8] G. Ploner, J. Smoliner, G. Strasser, M. Hauser, and E. Gornik, Phys. Rev. B 57, 3966 (1998).

[9] S. C. Lee, J. Y. Ryu, S. W. Kim, and C. S. Ting, Phys. Rev. B 62, 5045 (2000).

[10] S. C. Lee, D. S. Kang, J. D. Ko, Y. H. Yu, J. Y. Ryu, and S. W. Kim, J. Kor. Phys. Soc. 39, 643 (2001)

[11] G. -Q. Hai and F. M. Peeters, Phys. Rev. B 60, 16 513 (1999).

[12] D. J. Barnes, R. J. Nicholas, F. M. Peeters, X. G. Wu, J. T. Devreese, J. Singleton, C. J. G. M. Langerak, J. J. Haris, and C. T. Foxon, Phys. Rev. Lett. 66, 794 (1991).

[13] J. Y. Ryu, Y. C. Chung, and S. D. Choi, Phys Rev. B 32, 7769 (1985); J. Y. Ryu and S. D. Choi, Prog. Theor. Phys. 72, 429 (1984).

[14] S. D. Choi and O. H. Chung, Solid State Commun. 46, 717 (1983).

[15] P. N. Argyres and J. L. Sigel, Phys. Rev. B 10, 1139 (1974).

[16] I. S. Gradshteyn and i. M. Ryzhik, Tables of Integrals, Series and Products (Academic, New York, 1965).

[17] P. Vailopoulos, M. Charbonneau and C. M. Van Vliet, Phys. Rev. B 35, 1334 (1987).

[18] A. Suzuki and M. Ogawa, Phys. Rev. B 45, 6781 (1992).

[19] J. Singh, Physics of Semiconductors and Their Heterostructures (McGraw-Hill, Singapore, 1993).

[20] P. Y. Yu and M. Cardona, Fundamentals of Semiconductors (Springer, Berlin, New York, 1996).